

## Supplementary Material:

### Acoustic streaming induced by oscillating microbubbles in artificial crevices

Rocío Bolaños-Jiménez,<sup>1</sup> Massimiliano Rossi,<sup>2</sup> David Fernández-Rivas,<sup>3</sup> Christian J. Kähler,<sup>2</sup> and Alvaro Marin<sup>4</sup>

<sup>1</sup>Área de Mecánica de Fluidos, Departamento de Ingeniería Mecánica y Minera. Universidad de Jaén. Jaén, Spain.

<sup>2</sup>Institute for Fluid Mechanics and Aerodynamics, Bundeswehr University Munich, Germany

<sup>3</sup>MCS Group, Mesa +, University of Twente, The Netherlands

<sup>4</sup>Physics of Fluids, University of Twente, The Netherlands

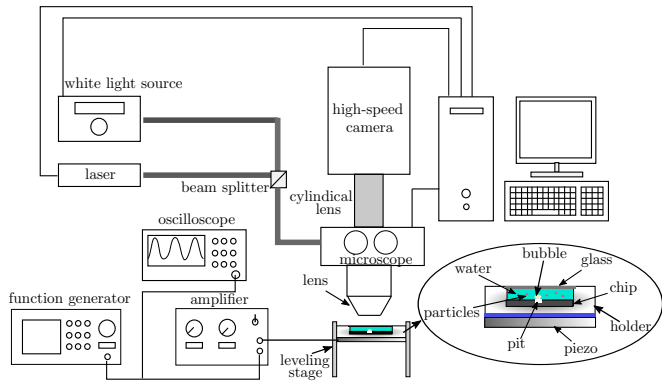


FIG. S1. General sketch of the experimental setup, including the optical arrangement, the illumination system, as well as the devices used to generate and control the ultrasound which was applied to the piezoelectric transducer. The latter was placed under the chip holder, whose details appear in the zoomed area.

#### I. EXPERIMENTAL DETAILS

Figure S1 shows a sketch of the complete experimental setup including all the components described in the main text. The chip was introduced in an aluminium holder (see Fig. S1) which contained a rectangular chamber of  $11 \times 11 \times 1$  mm that permitted to accommodate the chip and to fill the chamber completely with liquid using a precision syringe. In particular,  $\approx 300 \mu\text{l}$  of a solution of fluorescent spherical polystyrene particles (nominal diameter of  $1 \mu\text{m}$ , *Microparticles GmbH*) in ultrapure (*Milli-Q*) air-saturated water, was added into the chamber. A low concentration of particles ( $1:10^5$  in volume) was required in order to avoid particle overlaps during the recordings. The chamber was then closed by means of a thin cover glass (No. 1.5,  $180 \mu\text{m}$  thick), which allowed us to have optical access to the system. Extreme care was taken when closing the chamber in order to avoid that gas bubbles remained inside. The aluminium holder was attached to an ad-hoc leveling stage that permitted us to properly place the device under the upright microscope, as appearing in the picture shown in Figure S2(a).

The optimal position of the microscope was set by using white light illumination. In this way, the bubble interface could be observed (see Figure S2b) and centered in the image. Moreover, this illumination was used to check the bubble size after each experiment: if a change was observed, the experiment was restarted. To perform the

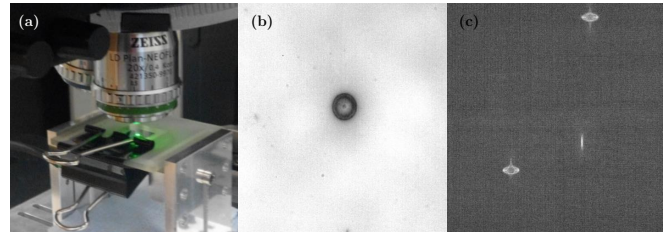


FIG. S2. (a) Picture of the setup under the microscope. (b) Image taken with white light, where the bubble interface can be observed. (c) Image taken with laser light and the cylindrical lens in front of the camera, where the spherical particles show the astigmatic effect.

experimental measurements, a continuous laser illumination was used instead. Figure S2(c) shows a typical image taken with the laser light and a filter to detect the fluorescent particles (bright areas). Moreover, the optical aberration introduced by the cylindrical lens over the particle's shape can be clearly noticed in this image. To correlate each elliptic shape with its depth-position, a sweep of images of the particles were taken along the depth distance (between  $50$  and  $100 \mu\text{m}$ , depending on the optical configuration) in steps of  $1 \mu\text{m}$ . The images were scaled using a *THORLABS* grid, getting spatial resolutions from  $0.24$  to  $0.29 \mu\text{m}/\text{pix}$ . Finally, in order to keep constant the temperature of the liquid as much as possible, the laser light was switched on only during the recording time. A *Pt1000* thermocouple was attached to the holder, close to the chamber, in order to register the temperature during the experiments, but a significant increase was not observed.

#### II. ACOUSTIC RESPONSE OF THE SYSTEM

Since the streaming flow generated by the oscillating bubble is studied in the frequency range from  $100$  to  $250$  kHz, we need to make sure that the system does not pass through a resonance in this range. This is done by performing a frequency scan and measuring the voltage required by the piezo-electric actuator. The result is shown in Figure S3, where the response of the complete system does not show any significant resonant peak within the studied frequency range.

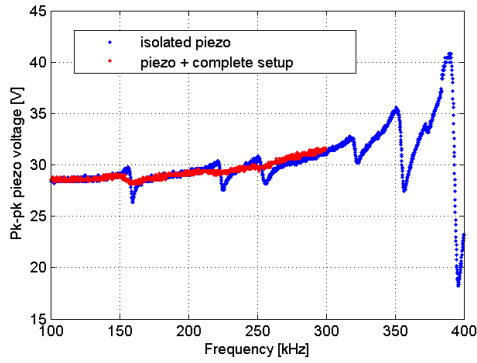


FIG. S3. Spectrum of the peak-to-peak voltage amplitude of the piezoelectric actuator under operative condition. The blue curve corresponds only to the isolated piezoelectric transducer, while the red curve is the result for the complete setup, including not only the piezoelectric transducer, but also the rest of the components of the experimental setup.

### III. BUBBLE STABILITY AT HIGHER DRIVING VOLTAGES

As mentioned in the main text, the increase of driving voltage also involved often a loss of symmetry of the flow pattern. An example is shown in Figure S4, which depicts two projections of the particle trajectories in the flow generated by an oscillating bubble driven at 150 kHz and 76 V<sub>pp</sub>. Note how the axial symmetry in the flow pattern is lost in the sense that particles approach the bubble from  $x > 0$  ( $u_r < 0$ ) and separate from the bubble for  $x < 0$  ( $u_r > 0$ ) (Fig. S4a). The flow pattern also is shown different in the  $x - z$  plane, where we can see

that all particles approach and separate from the bubble at comparable angles  $\theta$ , in stark contrast with the standard oscillation mode at lower voltages shown in the main text.

Since we are driving the bubble at its resonant frequency, we speculate that it probably becomes unstable easily as the driving amplitude is increased. It might be that by driving the bubble at a frequency different from the resonant one, one could obtain a larger range of voltages (or acoustic power) at which the bubble remains stable; but with substantially lower flow velocity.

### IV. INFLUENCE OF CONFINEMENT IN THE STREAMING FLOW

A consistent change in the streaming pattern can also be observed for bubbles oscillating at larger driving voltages under a confined environment. To illustrate this effect, FigureS4 shows a comparison of the particle trajectory obtained for the same experiment (fixed frequency and driving voltage) but placing the cover glass at a different height over the chip. In particular, Figures S4(a)-(b) show the particle trajectory measured when the glass cover slip was placed at  $\simeq 1000 \mu\text{m}$  from the bottom wall. This was the distance used to obtain the results shown in the main text. In Figures S4(c)-(d), a confinement was applied, being the cover glass placed at  $\simeq 100 \mu\text{m}$  from the bottom. In the latter case, it can be observed a very different trajectory pattern, in which particles entering at a certain angle remain trapped in horizontal loops, presenting some analogy with the quasi two-dimensional flow originated by cylindrical bubbles.

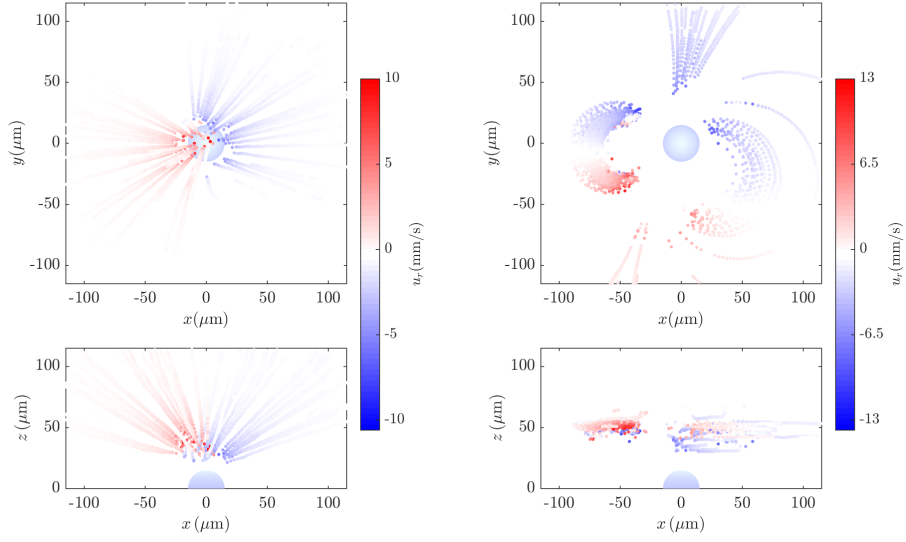


FIG. S4. (a)  $xy$  projection and (b)  $zx$  projection of particle trajectories of a bubble oscillating at  $f=150$  kHz and  $V_{pp}=76$  V showing abnormal flow patterns. Such patterns were often found at the resonant frequency 150 kHz and higher voltages. (c)  $xy$  projection and (d)  $zx$  projection of particle trajectories of a bubble oscillating at  $f=150$  kHz and  $V_{pp}=75$  V in a confined geometry, i.e. with the glass cover slip at  $\simeq 100 \mu\text{m}$  from the bottom wall. A consistent pattern with analogies to streaming flow originated by cylindrical bubbles can be observed.